



TITLE:

Geometric ferroelectricity in rare-earth compounds RGaO_3 and RInO_3

AUTHOR(S):

Tohei, Tetsuya; Moriwake, Hiroki; Murata, Hidenobu; Kuwabara, Akihide; Hashimoto, Ryo; Yamamoto, Tomoyuki; Tanaka, Isao

CITATION:

Tohei, Tetsuya ...[et al]. Geometric ferroelectricity in rare-earth compounds RGaO_3 and RInO_3 . PHYSICAL REVIEW B 2009, 79(14): 144125.

ISSUE DATE:

2009-04

URL:

<http://hdl.handle.net/2433/109878>

RIGHT:

© 2009 The American Physical Society

Geometric ferroelectricity in rare-earth compounds $RGaO_3$ and $RInO_3$

Tetsuya Tohei,^{1,*} Hiroki Moriwake,² Hidenobu Murata,¹ Akihide Kuwabara,² Ryo Hashimoto,¹ Tomoyuki Yamamoto,³ and Isao Tanaka^{1,2}

¹Department of Materials Science and Engineering, Kyoto University, Kyoto 606-8501, Japan

²Nanostructures Research Laboratory, Japan Fine Ceramics Center, Nagoya 456-8587, Japan

³Faculty of Science and Engineering, Waseda University, Tokyo 169-8555, Japan

(Received 30 October 2008; revised manuscript received 15 February 2009; published 30 April 2009)

We have studied the stability and ferroelectric properties of hexagonal $RGaO_3$ and $RInO_3$ (R : rare-earth elements) by first-principles calculations. Computed spontaneous polarization in the series shows a systematic increase with the rare-earth elements, with values being larger in $RInO_3$ than in the corresponding $RGaO_3$. The largest polarization found is about $10 \mu\text{C}/\text{cm}^2$ for $ErInO_3$, which is about twice as large as those observed in hexagonal $RMnO_3$. The polarization can be further increased by applying in-plane compressive stress. The Born effective charges of constituent ions in the compounds are found to be similar to their formal values, implying that the ferroelectric displacements are merely driven by the ionic size effect. A transition to the high-symmetry phase at around 1500 K was confirmed in $GdInO_3$ and $DyInO_3$ by *in situ* high-temperature powder x-ray diffractometry. The present systems should belong to the family of geometric ferroelectrics.

DOI: [10.1103/PhysRevB.79.144125](https://doi.org/10.1103/PhysRevB.79.144125)

PACS number(s): 77.80.-e, 77.84.Bw, 61.50.Ah

I. INTRODUCTION

A group of compounds with the hexagonal LuMnO_3 -type structure has attracted much attention because YMnO_3 and RMnO_3 (R : rare-earth element) families show the multiferroic property, i.e., the coexistence of magnetic ordering and ferroelectricity.¹⁻¹⁴ Although most studies in this field have focused on the correlation of magnetism and the dielectric property, the mechanism of ferroelectricity in such compounds is also interesting. First-principles calculations of YMnO_3 revealed that neither Y nor Mn shows anomalous dynamical charges associated with the atomic displacements that are typically found in conventional ferroelectric compounds.² Ferroelectricity in this compound was therefore attributed to the noncentrosymmetric atomic arrangement of the crystal caused merely by the ionic size effect, which is referred to as “geometric ferroelectricity.”^{2,3} Many of conventional ferroelectrics contain active cations such as Ti^{4+} , Nb^{5+} , and Ta^{5+} (so-called d^0 ions) or Pb^{2+} and Bi^{3+} (so-called s^2 lone-pair ions). Chemical bondings between these cations and neighboring anions play important roles in these ferroelectrics.^{2,15} The mechanism will hereafter be called the chemical bonding effect. Since the geometric ferroelectricity does not rely on special kinds of cations, an exploration of the geometric ferroelectrics should broaden research frontiers of ferroelectric materials. At the moment, however, both a systematic understanding of the nature of geometric ferroelectricity and a clear strategy for enhancing their properties are lacking. Values of the spontaneous polarization of the rare-earth manganites have been reported to be around $5\text{--}6 \mu\text{C}/\text{cm}^2$.¹⁶ However, one cannot find a clear trend in the variation of the ferroelectric properties of the compounds—spontaneous polarizations and ferroelectric Curie temperatures—in relation to the rare-earth elements. Furthermore, the idea of the geometric ferroelectricity in the compound has recently been still controversial.¹⁴

In the present study, we focus on a series of $RGaO_3$ and $RInO_3$ compounds having the hexagonal structure. The syn-

thesis of some $RGaO_3$ was reported in the mid-1970s.¹⁷ The compounds were found to be isostructural to LuMnO_3 with the space group of $P6_3cm$. The synthesis of hexagonal $RInO_3$ compounds was reported in the early 1960s.¹⁸ Later, they were confirmed to show the LuMnO_3 -type structure.¹⁹ The replacement of Mn by Ga, being almost the same in their ionic sizes, should provide an ideal material for the examination of the geometric effect on the structure of these systems, as magnetic or other electronic effects on crystal chemistry are eliminated. In fact, studies on the $\text{Y}(\text{Mn,Ga})\text{O}_3$ system showed that Ga substitution causes only small changes in the crystal structure or the ferroelectric Curie temperature of the compound.^{12,13} Studies of the $RInO_3$ system should reveal the effects of oversized ions at the Mn site of the structure. Although possible ferroelectricity in $RGaO_3$ and $RInO_3$ has been suggested in earlier reports,^{20,21} there have been no quantitative predictions or experimental confirmations made on their ferroelectric properties. In the present study, the structural and ferroelectric properties of these compounds are investigated by first-principles calculations, followed by experimental confirmation of the phase-transition behavior in $GdInO_3$ and $DyInO_3$.

II. METHODS

A. Computational method

First-principles total-energy calculations on the compounds were performed by a plane-wave basis projector augmented wave (PAW) method²² using the VASP code.^{23,24} The exchange and correlation effects were treated by the generalized gradient approximation (GGA).²⁵ In the potentials for lanthanide elements f electrons are kept frozen in the core. The k mesh was sampled according to the Monkhorst-Pack scheme²⁶ with a spacing of 0.3 \AA^{-1} . The cutoff energy in the plane-wave expansion was 500 eV. The convergence of relative energies with respect to the k mesh and energy cutoff was found to be better than 1 meV/atom. Structure optimi-

zations were performed allowing the relaxation of the unit-cell volume, cell dimensions, and fractional positions. The effect of in-plane compression in the hexagonal phase was calculated by imposing the constraint of a fixed lattice constant a . c -axis length at the condition was determined by calculating cells with several values of c length to draw energy versus c -length curve, obtaining the equilibrium value from the energy minima. The optimization of fractional positions was then performed with the fixed cell dimensions.

B. Sample preparation and x-ray diffraction measurements

Polycrystalline samples of GdInO_3 and DyInO_3 were synthesized by reacting an equimolar mixture of In_2O_3 (Kojundo Chemical Laboratory, 99.99%) and Gd_2O_3 or Dy_2O_3 (Rare Metallic, 99.9%) powders in air, respectively. Powders of these starting materials were mixed and ground in ethanol using a planetary ball mill (Fritsch P-7). Then the mixture was dried up, isostatically pressed into a pellet at 100 MPa, and sintered in air at 1623 K for 6 h. The compound thus prepared was examined by powder x-ray diffractometry and found to have a single phase of the desired hexagonal structure. Diffraction lines at room temperature were indexed by the hexagonal structure with the space group $P6_3cm$. Lattice constants of GdInO_3 and DyInO_3 at room temperature were determined to be $a=6.3462(1)$ Å, $c=12.3305(2)$ Å and $a=6.2915(1)$ Å, $c=12.2885(2)$ Å, respectively. High-temperature *in situ* measurements of powder x-ray diffraction were carried out up to 1573 K in air using Rigaku RINT-Ultima III with SHT1500 high-temperature attachment.

III. RESULTS AND DISCUSSION

A. Theoretical results for phase stability and spontaneous polarization

First we examine the relative stability of the hexagonal phase in these compounds against its competing phase of the perovskite structure. The existence of the hexagonal phase with the $P6_3cm$ space group has been reported for some RGaO_3 and RInO_3 .^{17,19} In these compounds, the hexagonal phase has been considered to compete with the perovskite phase.²⁷ Indeed, the occurrence of both phases has been reported in RGaO_3 and RInO_3 .^{17,19,28–31} In gallates, the orthorhombic perovskite phase (space group $Pnma$, GdFeO_3 -type structure) was obtained with rare-earth elements from La to Er,^{28–31} whereas the hexagonal phase was also reported with some late rare earths ($R=\text{Ho}$, Er , and Y).¹⁷ For indates, the perovskite phase was obtained with early rare earths of La, Nd, and Sm.^{31,32} The hexagonal phase was observed in middle to late rare-earth indates of $R=\text{Gd}$, Tb , Dy , and Ho .¹⁹ In ErInO_3 , a cubic solid solution with the bixbyite structure was obtained.¹⁹ On the whole, the hexagonal phase tends to be more stable than the perovskite phase in compounds with late rare earths, with a larger structural window in the indates series.

We have performed a series of total-energy calculations to investigate the relative stabilities of the perovskite and

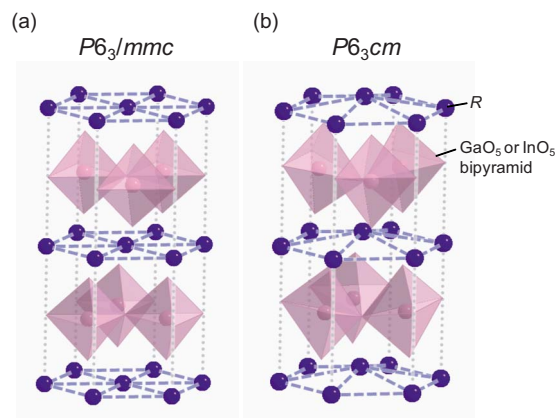


FIG. 1. (Color online) Schematic view of crystal structures of RGaO_3 and RInO_3 in the hexagonal structure. (a) High-symmetry ($P6_3/mmc$) phase. (b) Low-symmetry ($P6_3cm$) phase.

hexagonal phases. For the hexagonal phases, we considered a hypothetical high-symmetry phase with the space group of $P6_3/mmc$ in addition to the low-symmetry ferroelectric phase. The symmetry can be lowered from the $P6_3/mmc$ to the $P6_3cm$ phase in the hexagonal structure by tilting the BO_5 bipyramids and buckling the R layers, as depicted in Fig. 1. The calculation results of relative energies of different phases are presented in Fig. 2. The energy of the cubic perovskite phase [space group $Pm\bar{3}m$] is taken to be 0 eV as a reference. We can see that in RGaO_3 with early rare earths ($R=\text{Nd}$ and Sm), the perovskite phase has a lower energy than the hexagonal phase. In GdGaO_3 , the energies of the perovskite and hexagonal phases become almost the same, implying competing stability. As for gallates with later rare earths (Dy , Er), the hexagonal phase has a lower energy than the perovskite phase. On the other hand, in RInO_3 the hexagonal phase has a lower energy than the perovskite throughout the rare-earth series. The energy difference between the perovskite and the hexagonal phase becomes larger with the atomic number of rare-earth elements, indicating an increasing preference of the hexagonal phase over the perovskite counterpart. These calculated results are consistent with the experimentally observed tendencies of the phase stabilities in RGaO_3 and RInO_3 .

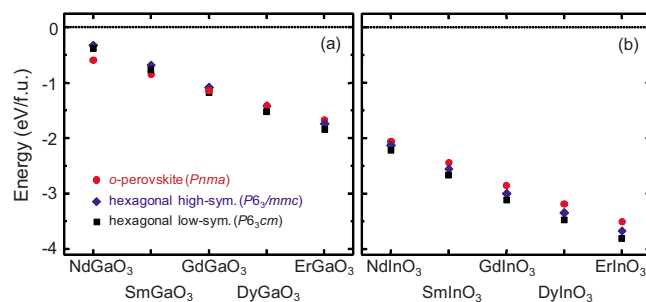


FIG. 2. (Color online) Relative energies of the different structures in the rare-earth compounds (a) RGaO_3 and (b) RInO_3 . The energy of the cubic perovskite phase is taken to be 0 eV as a reference. The energies of orthorhombic perovskite ($Pnma$) and high-symmetry ($P6_3/mmc$) and low-symmetry ($P6_3cm$) hexagonal phases are indicated by circles, diamonds, and squares, respectively.

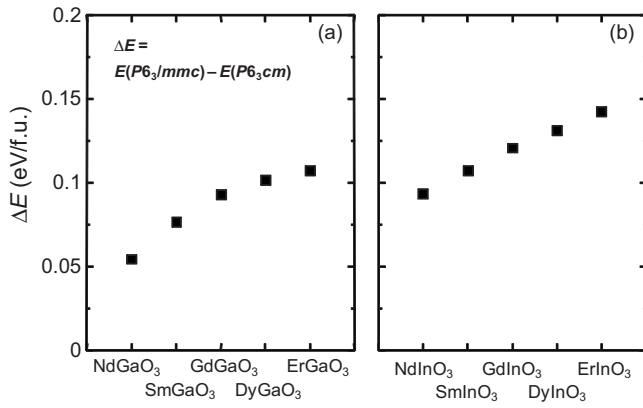


FIG. 3. Energy difference between the high-symmetry and low-symmetry hexagonal phases in (a) $RGaO_3$ and (b) $RInO_3$. The difference is obtained by subtracting the energy of the low-symmetry ($P6_3cm$) phase from that of the high-symmetry ($P6_3/mmc$) phase.

Within the hexagonal structures, the low-symmetry $P6_3cm$ phase always has lower energy than the high-symmetry $P6_3/mmc$ phase. The difference in the energy between $P6_3/mmc$ and $P6_3cm$ phases becomes larger with an increase in the atomic number of the rare-earth elements, as shown in Fig. 3. A larger energy difference is found in the indates than in the corresponding gallates. The energy difference between the high- and low-symmetry phases in $ErInO_3$ is about 1650 K. The value is much higher than the corresponding energy difference of 150 K in $BaTiO_3$ (between the cubic and the tetragonal structure).¹⁵ Although the energy difference at the ground states does not correspond to the transition temperature (because of neglecting the entropy contribution), the results may suggest that the ferroelectric Curie temperature or coercive field in the present system is much higher than those of $BaTiO_3$.

From the theoretically obtained crystal structures, one can evaluate the spontaneous polarization using displacements between the centrosymmetric and the noncentrosymmetric structures and ionic charges of constituents. Constituent ions are assumed to have either formal charges or Born effective charges. Calculated values of spontaneous polarizations for the series of compounds are shown in Fig. 4. The formal charges are taken as +3 for R , Ga , and In , and -2 for O , respectively. Born effective charges were calculated in the present study by Berry's phase approach.^{33,34} We found that the Born effective charges are close to the formal values and they bring about no significant enhancement in the polarization, as in the previously reported case of $YMnO_3$.^{2,35} This contrasts with the behavior of conventional ferroelectrics, such as $BaTiO_3$, where the Born effective charges are much larger than the formal charges.^{36,37} The ferroelectricity in $RGaO_3$ and $RInO_3$ can therefore be attributed to the noncentrosymmetric atomic arrangement driven by the geometric effect (or the ionic size effect) rather than the chemical bonding effect. The present system should be included in the family of geometric ferroelectrics.

In Fig. 4, a trend similar to that observed in the energy difference (Fig. 3) can be found in the change in the spontaneous polarization across the rare-earth gallates and indates. For the early $RGaO_3$ ($R=Nd$ and Sm), the obtained values

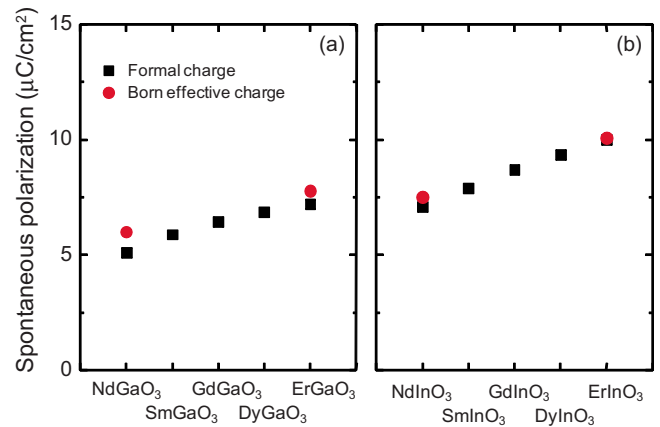


FIG. 4. (Color online) Calculated spontaneous polarizations of hexagonal (a) $RGaO_3$ and (b) $RInO_3$. Squares and circles show values calculated using formal charges and Born effective charges, respectively.

range from 5 to 6 $\mu C/cm^2$, which are close to the experimental values of hexagonal $YMnO_3$ and $RMnO_3$ reported previously.¹⁶ Although experimentally reported values of the spontaneous polarization of $RMnO_3$ show no clear trend relative to the rare-earth elements,¹⁶ the present calculated values of polarization show a systematic increase with the atomic number of rare-earth elements. The present results are reasonable if one recalls that the ferroelectricity in these compounds is brought about by a purely geometric effect. Rare-earth indates show larger polarization than the corresponding gallates. The maximum polarization of 10.0 $\mu C/cm^2$ is found in $ErInO_3$. This value for $ErInO_3$ is about twice as large as the experimentally observed value of $YMnO_3$. Previous analysis on $YMnO_3$ suggested that the dominant components of the structural distortion come from the out-of-plane (c -axis direction) displacements of the equatorial oxygen ions of MnO_5 bipyramid.² The decrease in R ion radius or increase in Ga/In site size makes the relatively small separation between Ga/In ions and equatorial oxygen ions more closer. This makes the equatorial oxygen ions feel more compressed by Ga/In ions within the c plane. The oxygen ions are therefore pushed away from the plane more strongly, resulting in larger displacements along c direction. Larger structural distortions should lead to larger polarizations or higher transition temperatures in the compounds.

Since the spontaneous polarization in these compounds occurs along the c axis of the crystal, one can expect that the application of the compressive stress within the ab plane or the elongation of the cell along the c axis will enhance their electric-dipole moment and therefore the spontaneous polarization. We investigate the effect of in-plane stress on the spontaneous polarization of these compounds. Compression was introduced to $ErInO_3$ by reducing the cell dimension a by -4% , 2% , 4% , 6% , or 8% from its equilibrium value. Such in-plane compression causes cell elongation along the c -axis direction. The dependence of the spontaneous polarization of $ErInO_3$ on the in-plane compression is depicted in Fig. 5. We can see that the in-plane compression enhances spontaneous polarization in the compound. An increase of about 80% in the polarization is achieved with an 8% reduc-

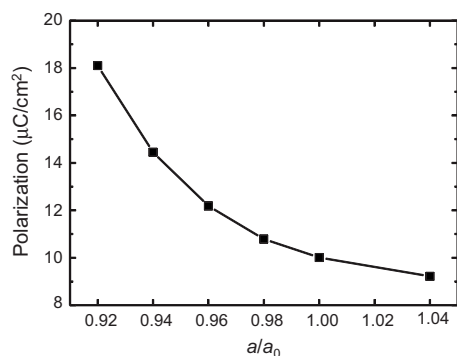


FIG. 5. Calculated dependence of the spontaneous polarization of ErInO_3 on the in-plane compression. The compression was along the direction of the ab plane.

tion of the cell dimension a . The polarization under this condition reaches about $18 \mu\text{C}/\text{cm}^2$, which is 3 times as large as those of uncompressed YMnO_3 and RMnO_3 families. This is the largest among the geometric ferroelectrics reported so far.^{2,38} These enhancements of the polarization may be attained by the physical pressure effect caused by the constraint from the substrate in epitaxially grown thin films or by the chemical pressure effect caused by doping or alloying with other materials of different ionic sizes of the constituents. The strategy applied to increase the polarization of ErInO_3 should be relevant to the control of the structural and ferroelectric properties of the other rare-earth gallates, indates, and manganites with the hexagonal LuMnO_3 -type structure.

B. Experimental phase transition

In order to confirm the occurrence of the low-symmetry (ferroelectric) to high-symmetry (paraelectric) phase transition experimentally, we have synthesized polycrystalline samples of compounds with the hexagonal structure and performed *in situ* measurements of powder x-ray diffraction at elevated temperatures. Among these RGaO_3 and RInO_3 , the desired hexagonal phase was successfully obtained for GdInO_3 and DyInO_3 . Attempts to synthesize late rare-earth gallates and early rare-earth indates under the same process conditions result in different phases other than the hexagonal structure. From our calculations, large polarization and high transition temperature close to the maximum value among these gallates and indates are expected in GdInO_3 and DyInO_3 .

The powder x-ray diffraction patterns of these two compounds recorded at room temperature and at elevated temperatures are shown in Fig. 6. A peak observed at around 33.0° – 33.5° (marked with filled circles) corresponds to the superlattice reflection in the low-symmetry $P6_3cm$ phase, which disappeared in the high-symmetry $P6_3/mmc$ phase. It is noted that the intensity of the superlattice reflection decreases with increasing temperature. The superlattice reflection disappears in both compounds in the diffraction patterns recorded at 1573 K. This suggests that the transition from the low-symmetry to the high-symmetry phase occurs at around this temperature. The transition temperature found here is the highest among the known isostructural RMO_3 families.^{16,21}

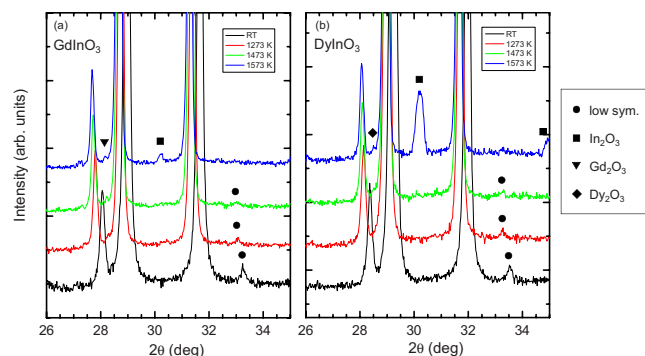


FIG. 6. (Color online) Powder x-ray diffraction patterns of (a) GdInO_3 and (b) DyInO_3 at RT and elevated temperatures. Superlattice reflection in the low-symmetry hexagonal phase is denoted by the circles. The peaks marked with squares, triangle, and diamond are assigned to In_2O_3 , Gd_2O_3 , and Dy_2O_3 , respectively.

We see new small peaks appearing in the patterns at 1573 K. The peaks marked with squares, triangle, and diamond are assigned to In_2O_3 , Gd_2O_3 , and Dy_2O_3 , respectively. All of these have the C-type rare-earth oxide (or the bixbyite-type) structure. They are probably products of the decomposition of the samples upon heating, indicating a limited stability of these hexagonal compounds at high temperatures in air. Similar sample decomposition to the present case has also been observed in the hexagonal manganites of YMnO_3 (Refs. 39 and 40) and LuMnO_3 .¹⁰

To summarize the experimental part, we have synthesized the hexagonal ferroelectric phase of GdInO_3 and DyInO_3 and confirmed the phase transition to the high-symmetry phase at around 1500 K. At the present moment, we are unable to synthesize the hexagonal phases in other RGaO_3 and RInO_3 compounds. Annealing the samples in air at above 1500 K induced the phase decomposition of GdInO_3 and DyInO_3 . By optimizing the process conditions, we may be able to observe the phase transition more clearly in a wider range of RGaO_3 and RInO_3 compounds. On the basis of the present theoretical calculations, lower ferroelectric Curie temperature and, therefore, a smaller barrier for polarization reversal can be expected in early RGaO_3 and RInO_3 . Ferroelectrics for practical uses should show reversible polarization upon applying external electric field near room temperature. This may be achieved in early RGaO_3 if the hexagonal structure can be synthesized. This may be accomplished in the form of thin films, as in the case of some RMnO_3 ,^{41,42} where the metastable hexagonal phases are difficult to obtain in the form of bulk materials. Then, the in-plane compressive stress can be applied by selecting an optimum substrate for increasing the spontaneous polarization.

IV. CONCLUSION

The stability and ferroelectric properties of a series of RGaO_3 and RInO_3 were investigated by first-principles calculations. The computed spontaneous polarization increased with increasing atomic number of rare-earth elements. RInO_3 showed larger polarization than the corresponding RGaO_3 . The largest polarization found in this study was about

10 $\mu\text{C}/\text{cm}^2$ for ErInO_3 , which is about twice as large as experimentally reported values of YMnO_3 and RMnO_3 families. Applying in-plane compressive stress was found to increase the polarization up to about 18 $\mu\text{C}/\text{cm}^2$ in ErInO_3 , indicating the enhancement of the polarization by a factor of about 3 relative to that of uncompressed YMnO_3 . The Born effective charges of constituent ions in RGaO_3 and RInO_3 were found to be similar to the formal charges. This implies that the origin of ferroelectricity in these compounds is different from that of conventional ferroelectrics such as BaTiO_3 in which the anomalous dynamic charge has been pointed out. The ferroelectricity can therefore be attributed to the noncentrosymmetric atomic arrangement of the crystal that is driven by the geometric effect rather than the chemical bonding effect. The present systems should belong to the family of geometric ferroelectrics. Finally, a transition from the low-symmetry to the high-symmetry phase was con-

firmed in GdInO_3 and DyInO_3 by *in situ* high-temperature powder x-ray diffractometry. The transition temperature was found to be at around 1500 K, which is the highest among the known isostructural RMO_3 compounds. These findings should provide a clue to the control of the structural and ferroelectric properties in this class of materials.

ACKNOWLEDGMENTS

The authors acknowledge Y. Ikuhara and T. Yamamoto of The University of Tokyo for helpful advice and support and K. Goto and H. Hayashi of Kyoto University for assistance in the experiments. This work was supported by a Grant-in-Aid for Scientific Research on Priority Areas "Nano Materials Science for Atomic Scale Modification 474" from the Ministry of Education, Culture, Sports, Science and Technology (MEXT) of Japan.

*Present address: Institute of Engineering Innovation, The University of Tokyo, Tokyo 113-8656, Japan.

- ¹M. Fiebig, Th. Lottermoser, D. Fröhlich, A. V. Goltsev, and R. V. Pisarev, *Nature (London)* **419**, 818 (2002).
- ²B. B. Van Aken, T. T. M. Palstra, A. Filippetti, and N. A. Spaldin, *Nature Mater.* **3**, 164 (2004).
- ³C. Ederer and N. A. Spaldin, *Nature Mater.* **3**, 849 (2004).
- ⁴T. Lottermoser, T. Lonkai, U. Amann, D. Hohenwein, J. Ihringer, and M. Fiebig, *Nature (London)* **430**, 541 (2004).
- ⁵R. Ramesh and N. A. Spaldin, *Nature Mater.* **6**, 21 (2007).
- ⁶S. Lee, A. Pirogov, M. Kang, K.-H. Jang, M. Yonemura, T. Kamiyama, S.-W. Cheng, F. Gozzo, N. Shin, H. Kimura, Y. Noda, and J.-G. Park, *Nature (London)* **451**, 805 (2008).
- ⁷N. A. Hill, *J. Phys. Chem. B* **104**, 6694 (2000).
- ⁸Z. J. Huang, Y. Cao, Y. Y. Sun, Y. Y. Xue, and C. W. Chu, *Phys. Rev. B* **56**, 2623 (1997).
- ⁹T. Katsufuji, S. Mori, M. Masaki, Y. Moritomo, N. Yamamoto, and H. Takagi, *Phys. Rev. B* **64**, 104419 (2001).
- ¹⁰Th. Lonkai, D. G. Tomuta, U. Amann, J. Ihringer, R. W. A. Hendrikx, D. M. Tobben, and J. A. Mydosh, *Phys. Rev. B* **69**, 134108 (2004).
- ¹¹C. J. Fennie and K. M. Rabe, *Phys. Rev. B* **72**, 100103(R) (2005).
- ¹²H. D. Zhou, J. C. Denysyn, and J. B. Goodenough, *Phys. Rev. B* **72**, 224401 (2005).
- ¹³U. Adem, A. A. Nugroho, A. Meetsma, and T. T. M. Palstra, *Phys. Rev. B* **75**, 014108 (2007).
- ¹⁴D. Y. Cho, J. Y. Kim, B. G. Park, K. J. Rho, J. H. Park, H. J. Noh, B. J. Kim, S. J. Oh, H. M. Park, J. S. Ahn, H. Ishibashi, S.-W. Cheong, J. H. Lee, P. Murugavel, T. W. Noh, A. Tanaka, and T. Jo, *Phys. Rev. Lett.* **98**, 217601 (2007).
- ¹⁵R. E. Cohen, *Nature (London)* **358**, 136 (1992).
- ¹⁶N. Fujimura, T. Ishida, T. Yoshimura, and T. Ito, *Appl. Phys. Lett.* **69**, 1011 (1996).
- ¹⁷S. Geller, J. B. Jeffries, and P. J. Curlander, *Acta Crystallogr., Sect. B: Struct. Crystallogr. Cryst. Chem.* **31**, 2770 (1975).
- ¹⁸S. J. Schneider, *J. Res. Natl. Bur. Stand.* **65A**, 429 (1961).
- ¹⁹C. W. F. T. Pistorius and G. J. Kruger, *J. Inorg. Nucl. Chem.* **38**, 1471 (1976).
- ²⁰S. C. Abrahams, *Acta Crystallogr., Sect. B: Struct. Sci.* **44**, 585 (1988).
- ²¹S. C. Abrahams, *Acta Crystallogr., Sect. B: Struct. Sci.* **57**, 485 (2001).
- ²²P. E. Blochl, *Phys. Rev. B* **50**, 17953 (1994).
- ²³G. Kresse and J. Furthmüller, *Phys. Rev. B* **54**, 11169 (1996); *Comput. Mater. Sci.* **6**, 15 (1996).
- ²⁴G. Kresse and D. Joubert, *Phys. Rev. B* **59**, 1758 (1999).
- ²⁵J. P. Perdew, K. Burke, and M. Ernzerhof, *Phys. Rev. Lett.* **77**, 3865 (1996).
- ²⁶H. J. Monkhorst and J. D. Pack, *Phys. Rev. B* **13**, 5188 (1976).
- ²⁷D. M. Giaquinta and H. C. Loye, *Chem. Mater.* **6**, 365 (1994).
- ²⁸S. Geller, *Acta Crystallogr.* **10**, 243 (1957).
- ²⁹S. Geller, P. J. Curlander, and G. F. Ruse, *Mater. Res. Bull.* **9**, 637 (1974).
- ³⁰J. C. Guitel, M. Marezio, and J. Mareschal, *Mater. Res. Bull.* **11**, 739 (1976).
- ³¹R. S. Roth, *J. Res. Natl. Bur. Stand.* **58**, 75 (1957).
- ³²S. J. Schneider, R. S. Roth, and J. L. Waring, *J. Res. Natl. Bur. Stand.* **65A**, 345 (1961).
- ³³R. D. King-Smith and D. Vanderbilt, *Phys. Rev. B* **47**, 1651 (1993).
- ³⁴R. Resta, *Rev. Mod. Phys.* **66**, 899 (1994).
- ³⁵As a typical example, calculated values of Born effective charges in hexagonal ErInO_3 are Er: +3.35, In: +3.34, O_{top} : -2.46, and O_{eq} : -1.77, respectively.
- ³⁶W. Zhong, R. D. King-Smith, and D. Vanderbilt, *Phys. Rev. Lett.* **72**, 3618 (1994).
- ³⁷Ph. Ghosez, J. P. Michenaud, and X. Gonze, *Phys. Rev. B* **58**, 6224 (1998).
- ³⁸C. Ederer and N. A. Spaldin, *Phys. Rev. B* **74**, 024102 (2006).
- ³⁹T. Katsufuji, M. Masaki, A. Machida, M. Moritomo, K. Kato, E. Nishibori, M. Takata, M. Sakata, K. Ohoyama, K. Kitazawa, and H. Takagi, *Phys. Rev. B* **66**, 134434 (2002).
- ⁴⁰I.-K. Jeong, N. Hur, and Th. Proffen, *J. Appl. Crystallogr.* **40**, 730 (2007).
- ⁴¹A. A. Bosak, C. Dubourdieu, J.-P. Senateur, O. Yu. Gorbenco, and A. R. Kaul, *J. Mater. Chem.* **12**, 800 (2002).
- ⁴²I. E. Graboy, A. A. Bosak, O. Yu. Gorbenco, A. R. Kaul, C. Dubourdieu, J.-P. Senateur, V. L. Svetchnikov, and H. W. Zandbergen, *Chem. Mater.* **15**, 2632 (2003).